


NANO EXPRESS

Open Access



Large-Area and Patternable Nano-Dot Array from Electrolysis of ITO Film for Surface-Enhanced Raman Spectroscopy

Han Lu^{1†}, Gengxin Han^{1†}, Jieping Cao¹, Mingliang Jin^{1,2*}, Qilin Ma³, Eser Metin Akinoglu², Xin Wang^{1,2}, Li Nian¹, Guofu Zhou^{1,2} and Lingling Shui^{1,2,3*} 

Abstract

Fabrication of large-area devices with patternable nanostructures is important for practical applications in optical or electrical devices. In this work, we describe an easy and environment-friendly method for preparing large-area nano-dot (ND) arrays via the electrolytic reaction of a metal oxide film. NDs with various size and morphology can be obtained by adjusting the applied voltage, electrolysis time, and the film thickness of the indium tin oxide (ITO) layer. High-density NDs with size of 50–60 nm can be obtained by electrolysis of a 25-nm-thick ITO film at 150 V for 1.5 min under a water droplet medium, which have been applied for surface-enhanced Raman spectroscopy (SERS) after depositing a thin layer of silver. The SERS substrate with optimized ND structure exhibits sensitive detection of Rhodamine 6G (R6G) with detection limit down to 5×10^{-12} M. The enhancement factors (EFs) of 1.12×10^6 and 6.79×10^5 have been achieved for characterization of 4-methylbenzenethiol (4-MBT) and R6G, respectively. With an additional photolithographic step, multiple areas of ND arrays can be created on one substrate, enabling simultaneous detection of various samples containing different molecules at once experiment. Such a method is quick, easy, patternable, and environment-friendly, being suitable for on-site quick and synchronous determination of various molecules for applications in point-of-care, environmental monitoring, and airport security fields.

Keywords: Nano-dot, SERS, Electrolysis, Array, High-throughput sensing

Introduction

Surface-enhanced Raman scattering (SERS) was observed a few decades ago from the roughed surface of silver electrode [1]. It has been widely investigated not only to understand the mechanism of SERS but also to achieve practical applications. Two classical series of SERS substrates have been developed, the self-assembled colloidal materials and the nanofabricated structures [2]. Nanoparticles of coinage metals like Ag, Au, and Cu have been synthesized for SERS studies [3, 4]. The nanoparticle systems are easy-to-use, however lack of repeatability and reproducibility with relatively low sensitivity [5, 6]. Nanostructures fabricated by e-

beam lithography [7, 8], laser interference lithography [9, 10], focused ion beam lithography [11], nanosphere lithography [12], and nanoimprint lithography [13] have shown high signal enhancement with excellent repeatability. However, these nanofabrication technologies require expensive equipment and restrict environment like ultraclean room; and the fabrication process is slow, as well.

Since SERS can be directly used for molecular sensing and identification in aqueous medium without interruption of water, it has been widely applied for small and biomolecular sensing [14–16]. For better and wider applications, easy and quick fabrication of SERS microarray substrate is still highly required for simultaneous detection of various molecules, especially for applications in point-of-care technology (POCT) and safety monitoring. Both colloidal particle assembly and nanofabrication technologies involve various types of chemicals or high energy consumption, for instance, special

* Correspondence: jinml@scnu.edu.cn; shuill@m.scnu.edu.cn

†Han Lu and Gengxin Han contributed equally to this work.

¹Guangdong Provincial Key Laboratory of Optical Information Materials and Technology, South China Academy of Advanced Optoelectronics, South China Normal University, Guangzhou 510006, China

Full list of author information is available at the end of the article

chemicals or gasses for particle synthesis and dry etch processes, respectively, and high energy consumption for sophisticated layer-by-layer design and deposition. Various environment unfriendly pollution are produced during the processes, such as organic, acid, base, heavy metal ions, and toxic etchant gas.

ITO films can be prepared via standard metal deposition technology and widely utilized in lab and industry as conductive substrate according to its transparency and low cost. Gao et al. have reported that ITO film could be transformed to indium (In) dots under cathodic polarization in NaOH solution [17].

In this work, we propose and verify a simpler, quicker, and greener technology by creating NDs on glass surface via direct electrolysis of ITO film in water in one step. With an additional photolithographic process, ND arrays can be created with patterned multiple separated areas and thus achieving simultaneous determination of multiple samples containing various types of molecules on one substrate. The electrolysis takes place under mild conditions at low voltage in water environment/medium.

Materials and Methods

Materials and Reagents

ITO glass (1.1-mm thick) was purchased from Luoyang Longqian Glass Co., Ltd. (Henan, China), with ITO thickness of 25, 50, 100, and 200 nm corresponding to the square resistance of 93.52, 31.05, 15.86, and 6.97 Ω /sq, respectively. Fluorine-doped tin oxide (FTO) glass (2.2-mm thick) was purchased from Yaoke Photoelectric Co., Ltd. (Jiangsu, China), with FTO thickness of 400 nm and square resistance of 10.85 Ω /sq. Deionized (DI) water (18.25 M Ω cm at 25 °C) was prepared using a Milli-Q Plus water purification system (Sichuan Wortel Water Treatment Equipment Co., Ltd., Sichuan, China). Ethanol (Damao Chemical Reagent Factory, Tianjin, China) and acetone (Zhiyuan Chemical Reagent Co., Ltd., Tianjin, China) were used to clean ITO glass. Photoresist SUN-120P was purchased from Suintific Microelectronic Materials Co., Ltd. (Shandong, China) for patterning ITO. 4-Methylbenzenethiol (4-MBT, 98%), sodium 2-mercaptoethanesulfonate (MESNa, \geq 98.0%) and dopamine hydrochloride were all purchased from Sigma-Aldrich (St. Louis, MO, USA). Rhodamine 6G (R6G, 98.5%) was purchased from J&K Scientific (Beijing, China). Potassium hydroxide (KOH, GR 95%) and melamine (99%) were purchased from Aladdin (Shanghai, China). D-(+)-Glucose (99%) was purchased from Alfa Aesar (Shanghai, China). Methylene blue (AR), urea (AR, \geq 99.0%) and phosphoric acid (AR, 85%) were purchased from Damao Chemical Reagent Factory (Tianjing, China). Formaldehyde solution (AR, 37–40%),

sodium dihydrogen phosphate dehydrate (AR, \geq 99.0%), and disodium hydrogen phosphate dodecahydrate (AR, \geq 99.0%) were purchased from Guangzhou Chemical Reagent Factory (Guangzhou, China). All chemicals were used as received.

Electrolysis of ITO Film in Water

An ITO glass substrate was first cut and cleaned sequentially in acetone, ethanol, and DI water, with each process lasting for 15 min, and then thoroughly rinsed with DI water and dried using nitrogen blowing. Figure 1 shows the schematic of the fabrication process. A droplet of DI water was dripped onto the ITO surface as the electrolysis medium. A wolfram (W) wire was inserted in the droplet and connected to the positive electrode, and ITO film was connected to the negative electrode of a power supplier (PSW800-1.44, GWINSTEK, Taiwan, China), as drawn in Fig. 1a. When a voltage was applied across the water, ITO was electrolyzed to form In NDs within the water medium area (Fig. 1b).

Moreover, an ITO film can be easily patterned to various areas in micrometer to centimeter range. An ITO film can also be patterned to an array with various isolated areas consisting NDs to achieve multiple functional areas on one substrate. This is very important for high-throughput/multiple detection devices. In order to form patterned ND arrays, 3.5 \times 3.5 cm² ITO-glass surface was patterned to separate square areas via a photolithography process. Afterwards, a grid-patterned ITO substrate and a flat ITO substrate were bonded face-to-face to form an in-parallel device sealed with 200- μ m-thick press adhesive frame and filled with DI water. The flat and patterned ITOs were connected to the positive and negative electrodes of a power supplier, respectively. This method was highly suitable for preparation of large-area and patterned ND arrays.

SERS Measurements

By tuning the applied voltage, electrolysis time, and ITO film thickness, the NDs' size and density could be varied. Formed NDs were typically tens to hundreds of nanometers arranged closely, forming nanogaps. A SERS substrate was then obtained by depositing a thin layer of Ag (PD400, Wuhan PDVACUUM Technologies Co., Ltd., Wuhan, China).

To characterize the sensitivity of such a SERS substrate, Raman spectra were measured using a Renishaw inVia Raman Microscope (Renishaw 42 K846, Renishaw Co., Ltd., UK). A SERS substrate was immersed into the analyte solution for 1 h and then thoroughly rinsed for 1 min using the corresponding solvent and blow dried with pure nitrogen gas. Dried SERS substrate was then placed on the stage of the Raman microscope for measurements. A 532 nm laser with a power of \sim 0.14 mW

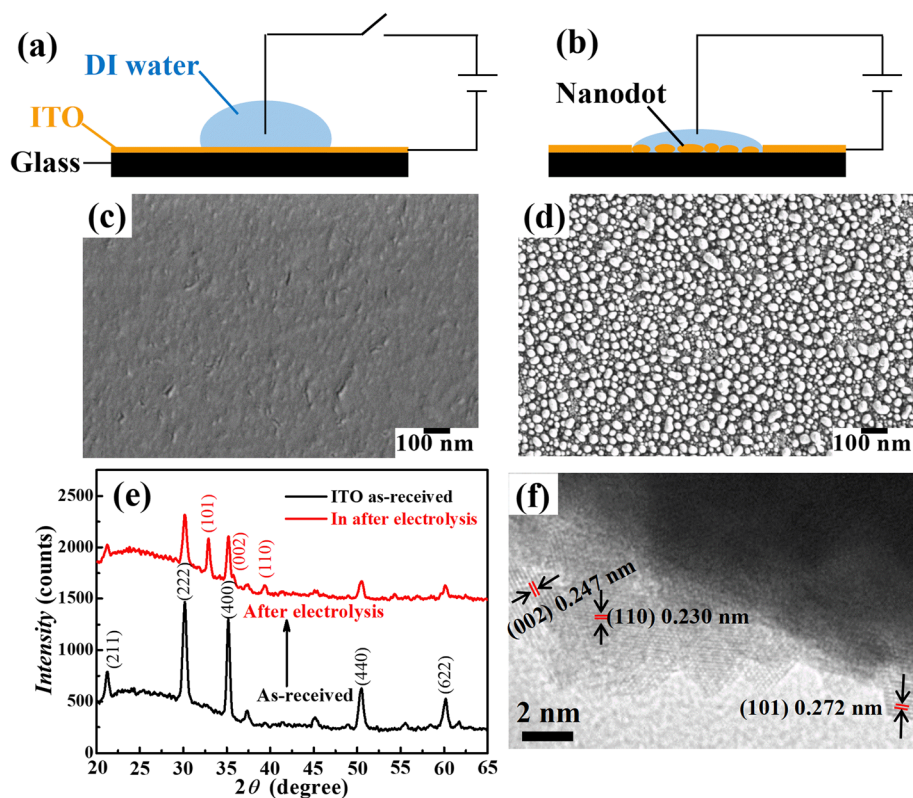


Fig. 1 Schematic of the In NDs formation from electrolysis of ITO film. **a** Initial state of a water droplet standing on an ITO film without applying a voltage. **b** Formation of NDs on the area covered with water when a voltage is applied. **c** SEM image of the intact ITO film surface corresponding to **a**. **d** SEM image of the formed NDs corresponding to **b** (applied voltage of 150 V for 1.5 min at ITO film thickness of 25 nm). **e** XRD spectra of the ITO film before and after electrolysis. **f** TEM image of the obtained In NDs

was focused on the sample through a $\times 50$ objective lens (numerical aperture, NA = 0.5, Leica). The diameter of the laser spot on substrate was 1.30 μm . The elastically scattered laser excitation was removed with an edge filter. Each Raman spectrum was collected with 10 s accumulation time.

Moreover, to evaluate the versatility and quick detection, nine probe molecules of 4-MBT, R6G, dopamine hydrochloride, urea, formaldehyde, methylene blue, MESNa, D-(+)-Glucose, melamine were chosen to characterize the prepared SERS substrate for simultaneous determination of multiple molecules. 4-MBT and methylene blue were dissolved in ethanol. MESNa was dissolved in DI water with pH of 2.7 tuned by the phosphate buffer solution. D-(+)-Glucose solution was prepared by using a phosphate buffer solution with pH of 7.5. All the rest sample solutions were prepared by dissolved in DI water. For each measurement, a droplet of 3.0 μL prepared solution was quickly dripped on the substrate, and the Raman spectrum was recorded immediately. The analyte concentrations were 10^{-4} , 5×10^{-11} , 10^{-3} , 0.5, 10^{-3} , 10^{-5} , 10^{-2} , 1, and 10^{-2} M for 4-MBT ethanol solution, R6G aqueous

solution, dopamine hydrochloride solution, urea aqueous solution, formaldehyde solution, methylene blue ethanol solution, MESNa solution, D-(+)-glucose solution, and melamine aqueous solution, respectively. All measurements were carried out immediately using the Raman instrument (Finder Insight, Zolix Instruments Co., Ltd., Beijing, China) with an excitation laser of 532 nm wavelength and 2.5 mW power. The 10- μm diameter laser beam was focused on the sample through a $\times 50$ objective (NA = 0.55). Each Raman spectrum was collected for 0.3 s/time, with 10 times accumulation.

Other Characterizations

The morphologies of fabricated substrate were characterized using a field emission-scanning electron microscopy (FE-SEM) (ZEISS-Ultra 55, Carl Zeiss AG, Germany) at an acceleration voltage of 5 kV. Transmission electron microscopy (TEM) measurements were carried out using a JEM-2100 microscopy (JEM-2100HR, JEOL, Japan). The nanodots (nanoparticles) were scraped and dispersed in DI water. Chemical composition was analyzed using an energy dispersive

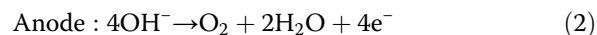
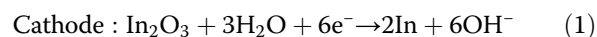
spectroscopy (EDS) equipped in the FE-SEM and an X-ray diffraction (XRD) (X'Pert PRO, PANalytical, The Netherlands) equipped with a Cu K α radiation source, at a scan rate of 0.04°/s, and the diffraction angle (2θ) from 20 to 65°. The absorption spectrum was recorded in the wavelength range of 440–650 nm by using a spectrometer (USB 2000+, Ocean Optics, USA).

Results and Discussion

Formation of Nanodots by Electrolysis of ITO Film in Water Medium

ITO films as transparent conductive substrates have been widely applied in optoelectronic devices such as light emission device (LED) [18], display [19], and solar cell [20]. In general, ITO corrosion is detrimental for electronic device applications. Here, on the other hand, we make use of the ITO corrosion induced by electrolysis reaction to form closely packed NDs and used for SERS application. Schematic of the electrolysis induced ND formation is shown in Fig. 1a, b. ITO film surface was flat and transparent before electrolysis (Fig. 1c). In general, ITO is a composed of In₂O₃ and SnO₂ in various proportion. EDS was carried out to characterize the composition of ITO, as shown in Additional file 1: Figure S1. After a period of electrolysis reaction, the ITO surface became translucent and yellow after drying. Characterized by SEM, we found that closely packed NDs on the glass surface were formed on the glass surface (Fig. 1d). XRD measurement in Fig. 1e shows that three new peaks appeared after electrolysis, which corresponds to (101), (002), and (110) crystal planes of In element. However, the peaks of ITO became lower. TEM image in Fig. 1f confirms that the formed NDs are of In material.

ITO film is a metal oxide material with morphologies of both crystalline and amorphous, with typically nanoscale surface roughness [21]. It has been reported that ITO can be corroded by NaOH to form In nanoparticles [17]. When a voltage is applied across the ITO film, electrons are transferred between cathode and anode. Therefore, the electrochemical reactions on cathode and anode can be described by Eqs. (1) and (2):



Therefore, the ND formation process can be illustrated in Fig. 2. In the beginning, the electrolysis reaction is homogeneous over the ITO surface. However, the ITO film is not perfectly homogeneous with film thickness variation existed according to normal ITO fabrication process, especially for amorphous ITO films [22]. Therefore, with time evolution, the thinner area will be consumed faster to form defects according to the higher electric field strength and smaller thickness. After reaching the saturation concentration in water, reduced In atoms start to accumulate to form NDs on surface. During the electrolysis, obvious transparency and color change could be observed after a period of time. According to the interfacial tension effect during a dewetting process, a large quantity of NDs was formed on the surface. Such a method, without any requirements for specific treatment and chemicals, is realized in water medium with an applied voltage and thus can be considered as an environment friendly technology.

Electrolysis Parameters: Reaction Time, Applied Voltage, and ITO Film Thickness

The NDs' size and density are related to the ITO film thickness and the reaction kinetics [23]. In this work, the effective factors of reaction time, applied voltage, and ITO film thickness were all investigated to find out the ND formation process. In this way, experimental parameters could be optimized to prepare SERS substrate with high sensitivity. Figure 3a shows the SEM images of obtained NDs on the glass (25-nm-thick ITO) at an applied voltage of 150 V at different reaction time. It obviously shows the sequential formation process from a continuous ITO film (Fig. 1c) to small NDs embedded in the film, rough NDs, smooth NDs, and standing and separated NDs, as demonstrated in the images in Fig. 3a from left to right, respectively. This gradual change in morphology and size can be understood by the electrolysis reaction of the ITO film and the diffusion-controlled ND formation process.

Initially, the ITO film started to react on the film surface. Typically, the electric field strength across the

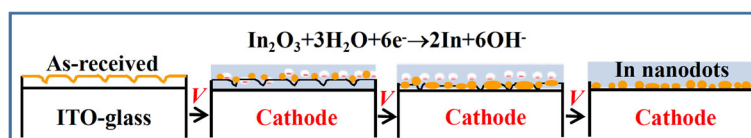


Fig. 2 Schematic illustration of the formation process of In NDs from electrolysis of ITO film

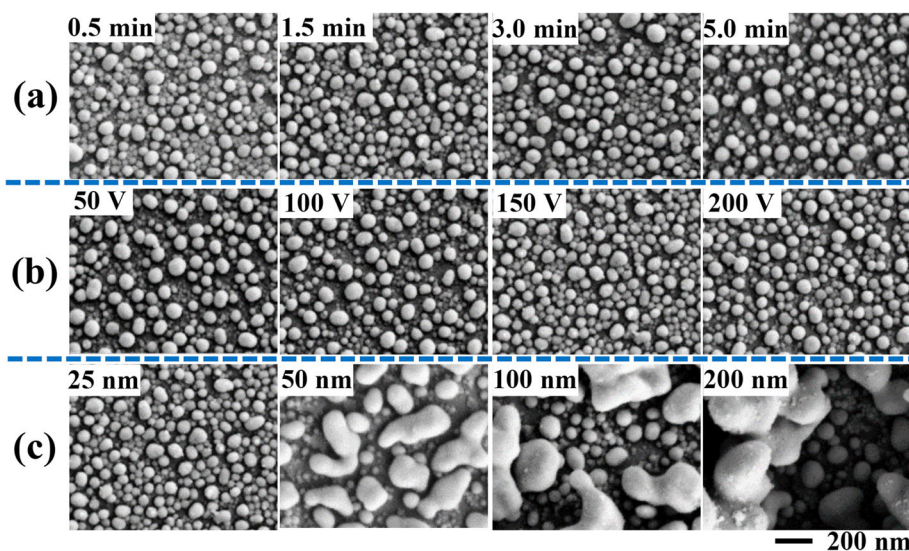


Fig. 3 Fabrication of NDs under various experimental conditions by varying **a** reaction time, at a constant applied voltage of 150 V and ITO film thickness of 25 nm, **b** applied voltage, at constant ITO film thickness of 25 nm and reaction time of 1.5 min, and **c** ITO film thickness, at constant applied voltage of 150 V and reaction time of 1.5 min

thinner area is higher; thus, the initial reaction speed is higher. Consequently, defects would form on the continuous film from the thin points (area), in which the produced In atoms accumulated to form NDs. At this stage, formed small NDs were still in the defect areas, being surrounded by the ITO film. With the increase of reaction time, most of ITO material was reduced to form In NDs on the surface. When the reaction time reached 0.5 min, large amount of NDs were formed, being embedded in the ITO film. When the reaction time increased to 1.5 min, the NDs' size and density increased, and the gap between NDs decreased. Further increasing the reaction time to 3.0 and 5.0 min, obtained NDs became larger and rounder, and the gap among NDs increased as well. Electrical measurements showed that the ND areas were not electrically conductive. This means that isolated NDs were obtained without continuous interconnection. From the SEM images in Fig. 3a, we could observe that, at the reaction time of 1.5 min, the formed NDs have relatively uniform size and arranged closely. Smaller gap usually means stronger electromagnetic enhancement. Thus, 1.5 min was selected for preparing the SERS samples for further experiments.

Afterwards, we investigated the effect of applied voltage on the size and density of formed NDs. An ITO-glass with a 25-nm-thick ITO has been chosen for this experiment, and an electrolysis reaction was carried out at different applied voltage for 1.5 min. As shown in Fig. 3b, the density of formed NDs increased with applied voltage. At low voltage of 50 and 100 V, the quantity of formed NDs was low; and thus, in the same area, its density was low, being obviously

separated to each other. When the applied voltage was increased to 150 and 200 V, more NDs were formed, showing closely arranged patterns. Uniform size and high density are essential to acquire reproducible Raman spectra with high sensitivity. Thus, the optimal applied voltage for SERS substrate preparation was set at 150 V.

Figure 3c shows the SEM images NDs formed from 25, 50, 100, and 200 nm ITO films by electrolysis reaction at 150 V for 1.5 min. In the case of 25 nm ITO film, higher density and more uniform NDs were observed compared with other three ITO films with thickness of 50, 100, and 200 nm. As reported, the surface roughness and resistivity of conductive substrates affect its crystallinity [22]. Typically, the surface roughness increases with film thickness. More uniform NDs from thinner ITO film were attributed to the more flat surfaces with fewer defects. Therefore, the thinnest ITO film exhibited the lowest roughness, resulting in the most uniform NDs. On the other hand, the resistivity of ITO films would influence the initial In ND formation process. The square resistance was 93.52, 31.05, 15.86, and 6.97 Ω/sq for the ITO film thickness of 25, 50, 100, and 200 nm, respectively. This means, at the same applied voltage, low electric current was obtained across the thin ITO film. As a result, slow and mild reaction was achieved on thin film. This is consistent with the experimental result that more uniform and higher density NDs were formed from the thinner ITO films. According to these results, the experimental parameters for preparing the NDs for SERS application were selected to be of ITO film thickness of 25 nm,

applied voltage of 150 V, and electrolysis reaction time of 1.5 min. Moreover, the FTO film has also been applied for electrolysis. As shown in Additional file 1: Figure S2, micro- and nano-particles formed after electrolysis. This may suggest that such an electrolysis reaction is also applicable for other metal oxide films at various conditions and potential for other applications.

SERS Characterization

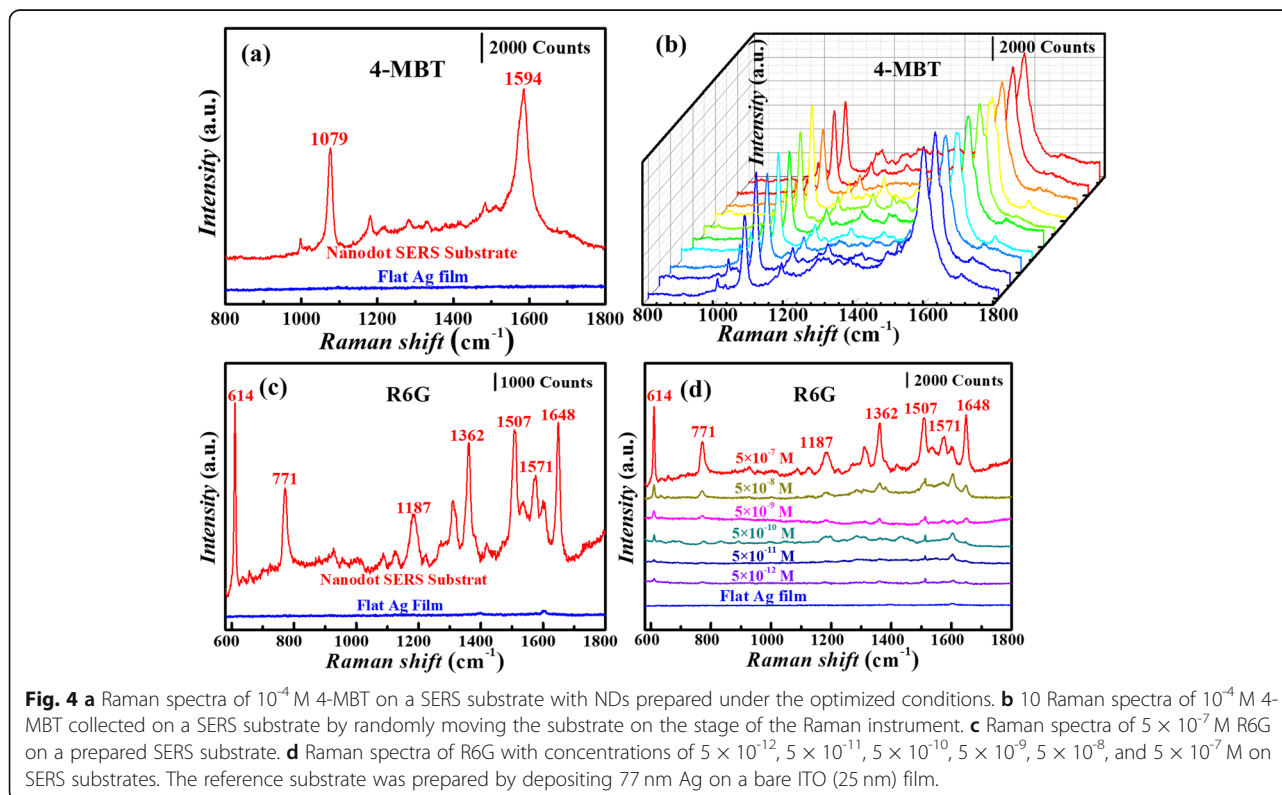
To evaluate SERS effect of the fabricated substrate with high density NDs, 4-MBT was selected as the probe molecule because of its small amount of well-characterized peaks and large Raman cross-section [24]. A thin layer of Ag was deposited on the obtained substrate (prepared under the optimized conditions as mentioned above) with high density NDs. SEM images in Additional file 1: Figure S3a–c show the morphologies of Ag covered NDs, at Ag layer thickness of 30, 77, and 160 nm, respectively. By varying the Ag layer thickness, the gaps between NDs decreased. The highest average Raman intensity was obtained at Ag thickness of 77 nm (Additional file 1: Figure S3d).

Figure 4a, b shows the detailed SERS characterization on the substrate with In NDs prepared under the optimized conditions and covered with 77 nm deposited Ag. The reference sample was prepared by directly depositing 77 nm Ag film onto an ITO (25 nm) glass. Raman signal was enhanced significantly on the ND SERS

substrate compared to the reference substrate. The two major characteristic peaks for 4-MBT molecules at 1079 and 1594 cm^{-1} were clearly observed on the ND SERS substrate. The 1079 cm^{-1} peak represents a combination of the phenyl ring-breathing mode, C–H in-plane bending and C–S stretching. The peak at 1594 cm^{-1} can be ascribed to phenyl stretching motion (8a vibrational mode) [25].

To investigate the relative homogeneity over a large area of the prepared ND SERS substrate, 10 measurements were carried out on the same substrate by randomly moving the sample on the stage of the Raman instrument. Figure 4b shows the measured Raman spectra, suggesting relatively consistent signal intensities for each characteristic peak of the 4-MBT. The relative standard deviation (RSD) of the Raman intensity at 1594 cm^{-1} was about 4.1%, indicating the high signal reproducibility of the SERS substrate prepared via this proposed process.

Moreover, R6G has also been selected to demonstrate the SERS substrate's reliability and sensitivity. Figure 4c shows the Raman spectra measured on an as-prepared ND SERS substrate and a reference Ag film. The characteristic peaks of R6G were observed at 614, 771, 1187, 1362, 1507, 1571, and 1648 cm^{-1} . The peaks at 614, 771, and 1187 cm^{-1} are ascribed to C–C–C ring in-plane bending, C–H out-of-plane bending, and C–O–C stretching vibrations, respectively. And the peaks at



1362, 1507, 1571, and 1648 cm^{-1} are associated with aromatic C–C stretching vibrations [26].

Figure 4d exhibits the Raman spectra on an as-prepared ND SERS substrate in R6G aqueous solution with concentrations ranging from 5×10^{-12} to 5×10^{-7} M. Raman intensities of R6G decreased obviously with the decrease of R6G concentration. The characteristic peaks of R6G could still be identified clearly even at the R6G concentration as low as 5×10^{-12} M, indicating the high sensitivity of the fabricated ND SERS substrate. To quantitatively characterize the SERS effect of prepared ND substrate, we have calculated the enhancement factor (EF). The Raman spectra of pure powders of 4-MBT and R6G (Additional file 1: Figure S4), and the detailed information of EF calculation (Additional file 1: Figure S5) are presented in the supplementary information. EFs for 4-MBT and R6G were calculated to be 1.12×10^6 and 6.79×10^5 at their characteristic Raman peaks of 1079 and 1648 cm^{-1} , respectively. Moreover, molecules with smaller Raman cross-section of MESNa [27] have also been used for SERS measurement, as shown in Additional file 1: Figure S6, demonstrating the reliable SERS effect.

In general, SERS enhancement can be contributed from electromagnetic (EM) and chemical (CM) effects [28]. Additional file 1: Figure S7 shows the absorption spectrum of ND substrate coated with 77 nm Ag film. The reference substrate was prepared by depositing 77 nm Ag on a bare ITO (25 nm) film. The NDs substrate was fabricated under the optimized experimental parameters of ITO film thickness of 25 nm, applied voltage of 150 V, and electrolysis reaction time of 1.5 min. When the excitation wavelength is the same as or close to the peak of surface plasmon resonance (SPR), the electromagnetic plasmonic coupling will take place and induce strong SERS enhancement [29]. The SPR peak of the NDs SERS substrate is at ~ 453 nm (Additional file 1: Figure S7), which is close to the excitation wavelength of 532 nm used in our experiment; therefore, the SERS enhancement is mainly resulted from the electromagnetic enhancement according to the “hotspots” from the inter-gaps between NDs. To further investigate the EM enhancement, finite-difference time-domain (FDTD) simulation was carried out to study the electric field in the inter-gaps of NDs. The results of relative total electric field are shown in Additional file 1: Figure S8. Simulation results show that the electric field enhancement mainly occurs at the gaps between NDs. The maximum factor of 3.0 represents a field enhancement $|E|^2$ of 10^3 corresponds to a EF of 10^6 , which is in good agreement with the experimental results (1.12×10^6 at 1079 cm^{-1} for 4-MBT and 6.79×10^5 at 1648 cm^{-1} for R6G).

Moreover, the semiconductor materials (In_2O_3 , SnO_2 , TiO_2) have been reported to enhance SERS signal by

charge transfer between the molecules and materials (e.g., R6G and transition metal oxides, 4-mercaptobenzoic (4-MBA)/4-nitrobenzenethiol (4-NBT), and SnO_2), which is related to CM [28, 30–33]. ITO is composed of In_2O_3 and SnO_2 in various proportion. After ITO electrolysis in water medium, the In NDs are formed due to the electrochemical reduction reaction; and at the same time, the peaks of ITO could still be observed obviously as shown in Fig. 1e. To investigate how much the CM enhancement from $\text{In}_2\text{O}_3/\text{SnO}_2$ -to-molecule charge transfer contributed to obtained SERS effect, the Raman spectra of 10^{-4} M 4-MBT and 5×10^{-7} M R6G on the ITO glass, NDs' substrate after ITO electrolysis, ITO glass coated with 77 nm Ag film, and NDs' substrate coated with 77 nm Ag film were measured, respectively (Additional file 1: Figure S9). The NDs' substrate was fabricated under the optimized experimental parameters of ITO film thickness of 25 nm, applied voltage of 150 V, and electrolysis reaction time of 1.5 min. The characteristic Raman peaks of 4-MBT and R6G were difficult to distinguish on the ITO glass, NDs substrate after ITO electrolysis, and ITO glass coated with Ag film; however, the obvious Raman peaks of 4-MBT and R6G were observed on NDs substrate coated with Ag film. Thus, the CM enhancement from $\text{In}_2\text{O}_3/\text{SnO}_2$ -to-molecule charge transfer is considered weak, being negligible comparing to EM enhancement. The highly enhanced SERS effect is mainly contributed from the electromagnetic enhancement between the inter-gaps between In NDs.

Patterned ND Arrays for Simultaneous SERS

Characterization of Various Samples on One Substrate

As demonstrated in the previous session, this method could easily create the NDs by a simple and quick electrolysis reaction on nanoscale ITO film. Moreover, an ITO film can be patterned by partially protecting or segmenting the film, thus forming arrays on one substrate, as schematically demonstrated in Fig. 5a. Three 3.5×3.5 cm^2 substrates have been patterned to 1×1 , 3×3 , and 5×5 SERS areas, as demonstrated in Fig. 5b. Since the ITO area for electrolysis reaction was enhanced compared to the droplet electrolysis, the total charge number increases during electrolysis, inducing the increase in current and decrease in resistance. According to the current limit of the power supplier of 1.512 A, the maximum output voltage of ~ 75 V has been applied for the In NDs preparation in the patterned in-parallel cells. The electrolysis time was investigated, as demonstrated in Additional file 1: Figure S10. The ND arrays with highest density and uniformity were obtained at the reaction time of 5.0 min. Here, the optimized parameters of ITO film thickness of 25 nm, applied voltage of 75 V, and electrolysis reaction time of 5.0 min were employed for fabricating the large area SERS substrate with

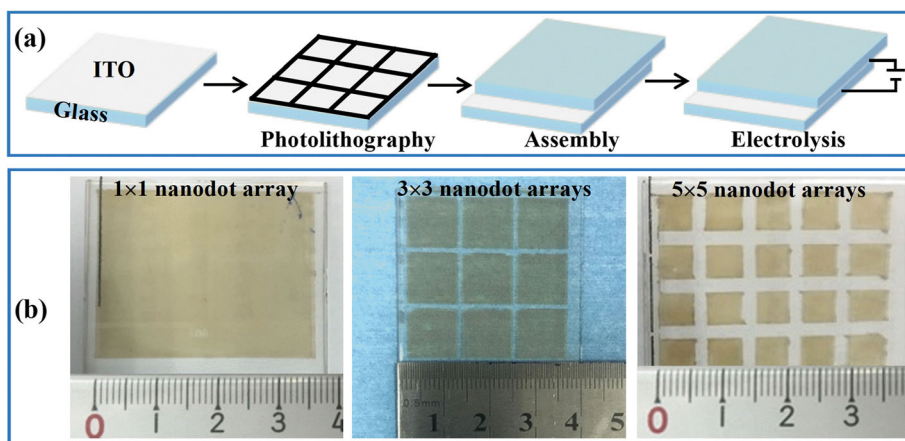


Fig. 5 **a** Schematic of patterning an ITO film to an array with multiple isolated areas containing NDs. **b** Images of the 1 × 1, 3 × 3, and 5 × 5 SERS arrays patterned from three 3.5 × 3.5 cm² ITO-glass substrates

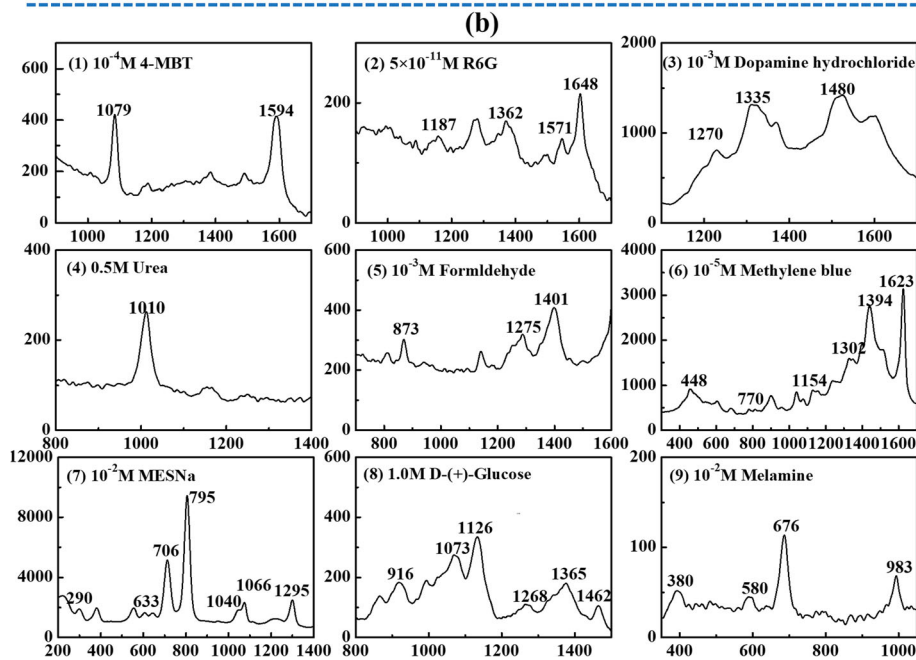
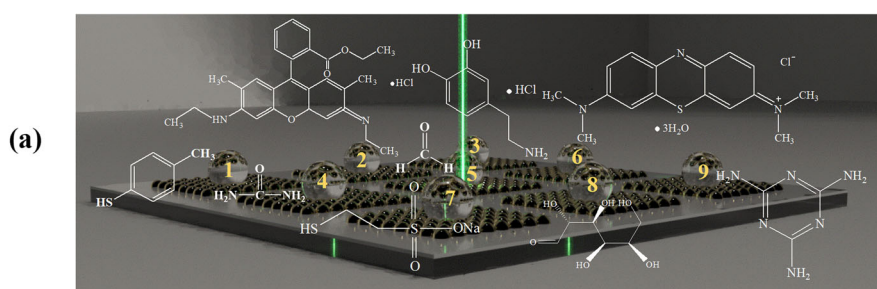


Fig. 6 **a** Schematic of 9 sample droplets containing 9 different probe molecules being detected on one substrate with a 3 × 3 SERS arrays. **b** Raman spectra of the 9 probe molecules on each SERS area of the 3 × 3 arrays

patterned ND arrays. The $50 \times 50 \mu\text{m}^2$ square ND arrays with gap distance of about $5.0 \mu\text{m}$ have been achieved, as shown in Additional file 1: Figure S11.

A substrate with 3×3 areas prepared under the optimized conditions was used as a SERS substrate for multiple sample detection. As illustrated in Fig. 6a, 9 individual droplets ($3.0 \mu\text{L}$ for each) containing 9 different analytic solutions were dripped at the patterned 9 areas. The selected 9 analytes 4-MBT [25], R6G [26], dopamine hydrochloride [34], urea [35], formaldehyde [36], methylene blue [37], MESNa [38, 39], D-(+)-Glucose [40], and melamine [41] were placed on the substrate as marked as samples 1 to 9, respectively. As seen from Fig. 6b, all 9 molecules show obvious Raman characteristic peaks. This has proven that the concept of using one substrate for simultaneously detection of various samples on one substrate.

Conclusions

In summary, we have proposed and validated a simple, quick, and cheap method for fabricating NDs as SERS substrates on large-area surface with patternable structures. The formation of NDs was based on electrolysis of ITO film in water medium. The factors of electrolysis time, applied voltage, and ITO film thickness determined the ND size and density. Well-distributed NDs with size in the range of 50–60 nm have been obtained by electrolysis a 25-nm-thick ITO film at an applied voltage of 150 V for 1.5 min (droplet electrolysis). The fabricated ND substrate has been evaluated by its SERS effect after depositing ~ 77 nm Ag, using various probe molecules. Reproducible and sensitive Raman spectra have been obtained for 4-MBT and R6G with EFs of $\sim 1.12 \times 10^6$ and $\sim 6.79 \times 10^5$, respectively. Moreover, combined with photolithography, a $3.5 \times 3.5 \text{ cm}^2$ substrate could be patterned with 1, 9, or 25 SERS areas, for which multiple sample detection could be achieved simultaneously on one substrate with just one droplet of each analytic solution. This is highly required for quick qualification of specific molecules for on-site application situations like POCT, environmental monitoring, and airport security check. Such a technology shows advantages of easy fabrication under mild conditions, being patternable to form arrays on a large surface, and being integratable with microfluidics for high throughput optofluidic applications.

Supplementary information

Supplementary information accompanies this paper at <https://doi.org/10.1186/s11671-019-3239-9>.

Additional file 1: Figure S1. EDS spectrum of ITO film. **Figure S2.** (a) SEM image of original FTO film. (b–e) SEM images of FTO film after electrolysis at different applied voltage 50, 100, 150 and 200 V, respectively.

Figure S3. SEM images of different Ag film thicknesses deposited on NDs (a) 30 nm, (b) 77 nm, (c) 160 nm. (d) Raman spectra of 10^{-4} M 4-MBT on NDs deposited with different Ag film thicknesses. **Figure S4.** (a) Raman spectra of 10^{-4} M 4-MBT on NDs SERS substrate and pure powder of 4-MBT on glass substrate, (b) Raman spectra of 5×10^{-7} M R6G on NDs SERS substrate and pure powder of R6G on glass substrate. **Figure S5.** Schematic to estimate the number of probe molecules trapped in the "hot-spot" area (N_{SERS}) among in the neighboring NDs. **Figure S6.** Raman spectra of 10^{-3} M MESNa on the NDs SERS substrate under the optimized conditions. **Figure S7.** Absorption spectrum of the NDs SERS substrate fabricated under optimized conditions. **Figure S8.** FDTD simulation of the electric field in the inter-gaps of NDs. **Figure S9.** Raman spectra of (a) 10^{-4} M 4-MBT and (b) 5×10^{-7} M R6G on ITO glass, NDs substrate after ITO electrolysis, ITO glass coated with 77 nm Ag film and NDs substrate coated with 77 nm Ag film, respectively. **Figure S10.** Fabrication of large area patterned ND arrays at different electrolysis time (a) 1.5 min, (b) 3.0 min, (c) 5.0 min, (d) 7.0 min, and (e) 10.0 min. **Figure S11.** SEM images of a patterned area after photolithography (a) before and (b) after electrolysis. SEM images of (c) the center and (d) the edge of a patterned ND area.

Abbreviations

4-MBA: 4-Mercaptobenzoic; 4-MBT: 4-Methylbenzenethiol; 4-NBT: 4-Nitrobenzenethiol; CM: Chemical effect; DI: Deionized; EDS: Energy dispersive spectroscopy; EF: Enhancement factor; EFs: Enhancement factors; EM: Electromagnetic effect; FDTD: Finite-difference time-domain; FE-SEM: Field emission-scanning electron microscopy; FTO: Fluorine-doped tin oxide; In: Indium; ITO: Indium tin oxide; KOH: Potassium hydroxide; LED: Light emission device; MESNa: Sodium 2-mercaptoethanesulfonate; ND: Nano-dot; POCT: Point-of-care technology; R6G: Rhodamine 6G; RSD: Relative standard deviation; SERS: Surface-enhanced Raman scattering; SERS: Surface-enhanced Raman spectroscopy; SPR: Surface plasmon resonance; TEM: Transmission electron microscopy; W: Wolfram; XRD: X-ray diffraction

Acknowledgements

Not applicable.

Authors' Contributions

MJ and LS designed the experiment and corrected the manuscript. HL and GH performed the experiment and drafted the manuscript. JC participated in the sample fabrication and characterizations. QM, EA, XW, LN, and GZ helped analysis experimental data and polish the manuscript. All authors have read and approved the final manuscript.

Funding

This research was funded by the National Key Research & Development Program of China (2016YFB0401502), the National Natural Science Foundation of China (61574065, 51561135014), Science and Technology Planning Project of Guangdong Province (2016B090906004), Special Fund Project of Science and Technology Application in Guangdong (2017B020240002), the Science and Technology Project of Guangdong Province (2018A050501012), and Guangdong Innovative and Entrepreneurial Team Program (2016ZT06C517). This work has also been partially supported by the PCSIRT Project No. IRT_17R40, the National 111 Project, the MOE International Laboratory for Optical Information Technologies, and the Guangdong Innovative Research Team Program (No. 2011D039).

Availability of Data and Materials

All data generated or analyzed during this study are included in this article.

Competing Interests

The authors declare that they have no competing interests.

Author details

¹Guangdong Provincial Key Laboratory of Optical Information Materials and Technology, South China Academy of Advanced Optoelectronics, South China Normal University, Guangzhou 510006, China. ²International Academy of Optoelectronics at Zhaoqing, South China Normal University, Zhaoqing 526238, China. ³School of Information and Optoelectronic Science and Engineering, South China Normal University, Guangzhou 510006, China.

Received: 27 September 2019 Accepted: 24 December 2019

Published online: 13 January 2020

References

- Jin RC (2010) Nanoparticle clusters light up in SERS. *Angew Chem Int Ed* 49(16):2826–2829
- Su D, Jiang SL, Yu MN, Zhang GZ, Liu H, Li MY (2018) Facile fabrication of configuration controllable self-assembled Al nanostructures as UV SERS substrates. *Nanoscale* 10(48):22737–22744
- Zhang C, Jiang SZ, Yang C, Li CH, Huo YY, Liu XY, Liu AH, Wei Q, Gao SS, Gao XG, Man BY (2016) Gold@silver bimetal nanoparticles/pyramidal silicon 3D substrate with high reproducibility for high-performance SERS. *Sci Rep UK* 6:25243
- Yang N, You TT, Liang X, Zhang CM, Jiang L, Yin PG (2017) An ultrasensitive near-infrared satellite SERS sensor: DNA self-assembled gold nanorod/nanospheres structure. *Rsc Adv* 7(15):9321–9327
- Banholzer MJ, Millstone JE, Qin LD, Mirkin CA (2008) Rationally designed nanostructures for surface-enhanced Raman spectroscopy. *Chem Soc Rev* 37(5):885–897
- La Porta A, Sanchez-Iglesias A, Altantzis T, Bals S, Grzelczak M, Liz-Marzan LM (2015) Multifunctional self-assembled composite colloids and their application to SERS detection. *Nanoscale* 7(23):10377–10381
- Patze S, Huebner U, Liebold F, Weber K, Cialla-May D, Popp J (2017) SERS as an analytical tool in environmental science: the detection of sulfamethoxazole in the nanomolar range by applying a microfluidic cartridge setup. *Anal Chim Acta* 949:1–7
- Jin ML, Pully V, Otto C, van den Berg A, Carlen ET (2010) High-density periodic arrays of self-aligned subwavelength nanopillars for surface-enhanced Raman spectroscopy. *J Phys Chem C* 114(50):21953–21959
- Quilis NG, Lequeux M, Venugopalan P, Khan I, Knoll W, Boujday S, de la Chapelle ML, Dostalek J (2018) Tunable laser interference lithography preparation of plasmonic nanoparticle arrays tailored for SERS. *Nanoscale* 10(21):10268–10276
- Jin ML, van Wolferen H, Wormeester H, van den Berg A, Carlen ET (2012) Large-area nanogap plasmon resonator arrays for plasmonics applications. *Nanoscale* 4(15):4712–4718
- Sivashanmugan K, Liao JD, You JW, Wu CL (2013) Focused-ion-beam-fabricated Au/Ag multilayered nanorod array as SERS-active substrate for virus strain detection. *Sens Actuators B Chem* 181:361–367
- Zhao XY, Wen JH, Zhang MN, Wang DH, Chen YWL, Chen L, Zhang Y, Yang J, Dut Y (2017) Design of hybrid nanostructural arrays to manipulate SERS-active substrates by nanosphere lithography. *ACS Appl Mater Interfaces* 9(8):7710–7716
- Lee KL, Hung CY, Pan MY, Wu TY, Yang SY, Wei PK (2018) Dual sensing arrays for surface plasmon resonance (SPR) and surface-enhanced Raman scattering (SERS) based on nanowire/nanorod hybrid nanostructures. *Adv Mater Interfaces* 5(21):1801064
- Gong TX, Cui Y, Goh D, Voon KK, Shum PP, Humbert G, Auguste JL, Dinh XQ, Yong KT, Olivo M (2015) Highly sensitive SERS detection and quantification of sialic acid on single cell using photonic-crystal fiber with gold nanoparticles. *Biosens Bioelectron* 64:227–233
- Karadan P, Aggarwal S, Anappara AA, Narayana C, Barshilia HC (2018) Tailored periodic Si nanopillar based architectures as highly sensitive universal SERS biosensing platform. *Sens Actuators B Chem* 254:264–271
- Zhang SD, Xiong R, Mahmoud MA, Quigley EN, Chang HB, El-Sayed M, Tsukruk W (2018) Dual-excitation nanocellulose plasmonic membranes for molecular and cellular SERS detection. *ACS Appl Mater Interfaces* 10(21):18380–18389
- Gao WJ, Cao S, Yang YZ, Wang H, Li J, Jiang YM (2012) Electrochemical impedance spectroscopy investigation on indium tin oxide films under cathodic polarization in NaOH solution. *Thin Solid Films* 520(23):6916–6921
- Pan CF, Dong L, Zhu G, Niu SM, Yu RM, Yang Q, Liu Y, Wang ZL (2013) High-resolution electroluminescent imaging of pressure distribution using a piezoelectric nanowire LED array. *Nat Photonics* 7(9):752–758
- Li ZH, Cho ES, Kwon SJ (2010) Laser direct patterning of the T-shaped ITO electrode for high-efficiency alternative current plasma display panels. *Appl Surf Sci* 257(3):776–780
- Chu AK, Tien WC, Lai SW, Tsai HL, Bai RY, Lin XZ, Chen LY (2017) High-resistivity sol-gel ITO thin film as an interfacial buffer layer for bulk heterojunction organic solar cells. *Org Electron* 46:99–104
- Cheng CW, Chen JS, Chen HH (2010) Patterning of crystalline ITO using infrared nanosecond fiber laser pulses. *Mater Manuf Process* 25(7):684–688
- Li X, Li CY, Hou SW, Hatta A, Yu JH, Jiang N (2015) Thickness of ITO thin film influences on fabricating ZnO nanorods applying for dye-sensitized solar cell. *Compos Part B-Eng* 74:147–152
- Markina NE, Markin AV, Zakharevich AM, Goryacheva IY (2017) Calcium carbonate microparticles with embedded silver and magnetite nanoparticles as new SERS-active sorbent for solid phase extraction. *Microchim Acta* 184(10):3937–3944
- Jin ML, Zhu YF, van den Berg A, Zhang Z, Zhou GF, Shui LL (2016) Wafer-scale fabrication of high-density nanoslit arrays for surface-enhanced Raman spectroscopy. *Nanotechnology* 27(49):49LT01
- Li WY, Camargo PHC, Lu XM, Xia YN (2009) Dimers of silver nanospheres: facile synthesis and their use as hot spots for surface-enhanced Raman scattering. *Nano Lett* 9(1):485–490
- Jayaram ND, Aishwarya D, Sonia S, Mangalaraj D, Kumar PS, Rao GM (2016) Analysis on superhydrophobic silver decorated copper oxide nanostructured thin films for SERS studies. *J Colloid Interf Sci* 477:209–219
- Wang J, Jin ML, Gong YX, Li H, Wu SJ, Zhang Z, Zhou GF, Shui LL, Eijkel JCT, van den Berg A (2017) Continuous fabrication of microcapsules with controllable metal covered nanoparticle arrays using droplet microfluidics for localized surface plasmon resonance. *Lab Chip* 17(11):1970–1979
- Jiang L, Yin PG, You TT, Wang H, Lang XF, Guo L, Yang SH (2012) Highly reproducible surface-enhanced Raman spectra on semiconductor SnO₂ octahedral nanoparticles. *Chemphyschem* 13(17):3932–3936
- Liu GQ, Li Y, Duan GT, Wang JJ, Liang CH, Cai WP (2012) Tunable surface plasmon resonance and strong SERS performances of Au opening-nanoshell ordered arrays. *ACS Appl Mater Interfaces* 4(1):1–5
- Han XX, Ji W, Zhao B, Ozaki Y (2017) Semiconductor-enhanced Raman scattering: active nanomaterials and applications. *Nanoscale* 9(15):4847–4861
- Hou XY, Fan XC, Wei PH, Qiu T (2019) Planar transition metal oxides SERS chips: a general strategy. *J Mater Chem C* 7(36):11134–11141
- Agrawal A, Cho SH, Zandi O, Ghosh S, Johns RW, Milliron DJ (2018) Localized surface plasmon resonance in semiconductor nanocrystals. *Chem Rev* 118(6):3121–3207
- Kanehara M, Koike H, Yoshinaga T, Teranishi T (2009) Indium tin oxide nanoparticles with compositionally tunable surface plasmon resonance frequencies in the near-IR region. *J Am Chem Soc* 131(49):17736–17737
- Qin LX, Li XQ, Kang SZ, Mu J (2015) Gold nanoparticles conjugated dopamine as sensing platform for SERS detection. *Colloids Surf B Biointerfaces* 126:210–216
- Saini A, Medwal R, Bedi S, Mehta B, Gupta R, Maurer T, Plain J, Annapoorni S (2015) Axonic Au tips induced enhancement in Raman spectra and biomolecular sensing. *Plasmonics* 10(3):617–623
- Zhang ZM, Zhao C, Ma YJ, Li GK (2014) Rapid analysis of trace volatile formaldehyde in aquatic products by derivatization reaction-based surface enhanced Raman spectroscopy. *Analyst* 139(14):3614–3621
- Li CY, Huang YQ, Lai KQ, Rasco BA, Fan YX (2016) Analysis of trace methylene blue in fish muscles using ultra-sensitive surface-enhanced Raman spectroscopy. *Food Control* 65:99–105
- Piotrowski P, Bukowska J (2015) 2-Mercaptoethanesulfonate (MES) anion-functionalized silver nanoparticles as an efficient SERS-based sensor of metal cations. *Sens Actuators B: Chem* 221:700–707
- Chen Y, Wu LH, Chen YH, Bi N, Zheng X, Qi HB, Qin MH, Liao X, Zhang HQ, Tian Y (2012) Determination of mercury(II) by surface-enhanced Raman scattering spectroscopy based on thiol-functionalized silver nanoparticles. *Microchim Acta* 177(3–4):341–348
- Lyandres O, Yuen JM, Shah NC, VanDuyne RP, Walsh JT, Glucksberg MR (2008) Progress toward an in vivo surface-enhanced Raman spectroscopy glucose sensor. *Diabetes Technol The* 10(4):257–265
- Giovannozzi AM, Rolle F, Segal M, Abete MC, Marchis D, Rossi AM (2014) Rapid and sensitive detection of melamine in milk with gold nanoparticles by surface enhanced Raman scattering. *Food Chem* 159:250–256

Publisher's Note

Springer Nature remains neutral with regard to jurisdictional claims in published maps and institutional affiliations.